International Journal of Non-Linear Mechanics 73 (2015) 85–93

Contents lists available at ScienceDirect

International Journal of Non-Linear Mechanics

journal homepage: www.elsevier.com/locate/nlm

Chaotic behavior of a body in a resistant medium

Vladimir S. Aslanov

Theoretical Mechanics Department, Samara State Aerospace University, Samara, Russia

ARTICLE INFO

Article history:
Received 9 February 2014
Received in revised form
14 August 2014
Accepted 3 November 2014
Available online 13 November 2014

Keywords:
Rigid body
Resistant medium
Biharmonic torque
Chaos
Melnikov method

ABSTRACT

We study the pitch motion dynamics of a rigid body in a resistant medium under the influence of a biharmonic torque $a\sin\theta + b\sin 2\theta$. Such nutation angle dependence of the biharmonic aerodynamic torque is typical for uncontrolled re-entry vehicles of segmentally conical, blunted conical, and other shapes (Soyuz, Mars, Apollo, Viking, Galileo Probe, Dragon). The presence of the second harmonic in the biharmonic torque is the cause of additional unstable equilibrium. In case of spatial motion a small perturbation is a small difference of the transverse inertia moments of the body. In this case, two Euler angles $\theta$and ψ are the positional coordinates, and we can observe a chaos. In case of the planar motion the body is perturbed by a small aerodynamic damping torque and a small periodic torque of time. We show by means of the Melnikov method that the system exhibits a transient chaotic behavior. This method gives us an analytical criterion for heteroclinic chaos in the planar motion and an integral criterion for the spatial motion. The results of the study can be useful for studying the chaotic behavior of a spacecraft in the atmosphere.

1. Introduction

The dynamics of rotating bodies is a classic topic of study in mechanics. In the eighteenth and nineteenth centuries, several aspects of the motion of a rotating rigid body were studied by such famous mathematicians as Euler, Cauchy, Jacobi, Poinsot, Lagrange, and Kovalevskaya. In some cases, for the study of dynamical systems it can be useful to use elements of mathematical phenomenology and phenomenological approximate mappings for obtaining approximate differential equations and approximate solutions in local area around singular points, linear and non-linear approximations [1–2]. However, the study of the dynamics of rotating bodies is still very important for numerous applications such as the dynamics of satellite gyrostat, spacecraft, re-entry vehicle, and the like. Note that only some of the papers are devoted to the modern problem of rigid body dynamics. So in an independent way, Sadov [3] first obtained sets of action-angle variables for the rotational motion of a triaxial rigid body. Deprit and Elipe [4] used Sadov's variables to convert directly the Serret–Andoyer variables [5–7] into action-angle variables, thereby making Hamiltonian dependent on only two momenta. Akulenko et al. [8] considered perturbed motion about a fixed point of a dynamically symmetrical heavy solid in a medium with linear dissipation and obtained an averaged system of equations. Yaroshevskii created fundamentals of the dynamics of re-entry vehicles, which were used for designing the Soviet spacecraft such as Vostok, Souz, Luna, Venera and Mars. Yaroshevskii wrote two books in Russian and a large number of articles on this problem the latter of which [9–12]. Aslanov [13] studied the motion of a rotating rigid body in the atmosphere of a planet under the action of a restoring torque which depends on time and the angle of nutation. The rigid body (re-entry vehicle) intended to descend into the atmosphere usually has a small aerodynamic and dynamic asymmetry, for example, it has a small relative difference between the transverse moments of inertia [14]. In this case, the angular motion depends on two Euler angles: the nutation angle θ (spatial angle of attack) and the angle of spin ψ. If the frequency of change of these angles becomes multiple to the relation of simple integers, then a parametrical resonance occurs [14]. Holmes and Marsden applied the methods of chaotic dynamics [15] for solving a similar problem. Holmes and Marsden considered the problem of spatial motion of the heavy rigid body with a small dynamic asymmetry when the torque of gravity was proportional to $m_\theta \sim \sin\theta$. Similar tasks have also been discussed in the papers [16–19].

This paper focuses on the study of the motion of a blunt rigid body in an atmosphere which is under the action of a biharmonic aerodynamic torque $a\sin\theta + b\sin 2\theta$. The purpose of the paper is the finding of the conditions of existence of chaos in motion in the slightly asymmetrical rigid body in the atmosphere under the action of small perturbations and determining the influence of chaos on the behavior of the rigid body.

The paper is divided into five sections. In Section 2 the statement of the problem is given. In Section 3 the spatial motion of the slightly asymmetrical rigid body about its center of mass in an atmosphere is considered. An aerodynamic torque on the body

E-mail address: aslanov@ssau.ru

http://dx.doi.org/10.1016/j.ijnonlinmec.2014.11.002
0020-7462/

is determined by the biharmonic dependence on the angle of nutation. Hamilton's canonical equations are derived and conditions are found for the existence of unstable equilibria of the system. Homoclinic orbits are determined in an analytical form and Melnikov function is constructed in the modification of Holmes and Marsden [15]. Numerical simulation of a chaotic behavior of the system completes the section. In Section 4 we find an exact analytical representation of the Melnikov function for the planar motion, if the small disturbance is determined as the sum of a periodic time function and a dissipative torque. The analytical results given by the Melnikov method have been confirmed by a good agreement with direct numerical calculations in the construction of Poincaré sections by using the fourth-order Runge–Kutta algorithms. In Section 5, it is concluded that the biharmonic system will exhibit a lot of chaotic motions due to the combined physical parameters with external torques that are dissipative and periodic or due to the small dynamic asymmetry.

2. Problem formulation

Let's determine a place of the considered problem in the general problem of rigid body dynamics and also note an analogy to the motion of a heavy rigid body and the rigid body in the resisting medium (atmosphere of a planet). Gravity and aerodynamic torques acting on the sphere with a displaced center of mass in the resisting medium are proportional to $\sin\theta$ (Fig. 1a and b). The shape of the Soviet spacecraft Vostok was a sphere. On board Vostok, Soviet cosmonaut Yuri Gagarin made history on April 12, 1961, when he became both the first person in the world to enter space and to return to Earth. However, the modern re-entry vehicles have a blunted conical shape (Apollo, Galileo Probe, Dragon), it is to provide efficient braking in the atmosphere. For these re-entry vehicles (Fig. 1c) the aerodynamic torque is well approximated by biharmonic dependence on the nutation angle

$$m_\theta = a' \sin\theta + b' \sin 2\theta \tag{1}$$

However, the dependences on the angle of nutation (1) can have three positions of equilibrium, and one of them is unstable. The stable position at the points $\theta_* = 0$ and $\theta_* = \pi$; and unstable in the third intermediate point $\theta_* \in (0,\pi)$ [13,20,21]. The presence of the second harmonic in (1) causes the possibility of appearance of an additional equilibrium position – saddle point on a phase portrait. For the considered spacecraft position $\theta = 0$ is stable; therefore, a derivative of the function $m_\theta(\theta)$ with respect to the angle θ at this point is negative

$$\left.\frac{dm_\theta}{d\theta}\right|_{\theta=0} = (a'\cos\theta + 2b'\cos 2\theta)|_{\theta=0} < 0 \tag{2}$$

or

$$2b' < -a' \tag{3}$$

And if there exists an intermediate position of equilibrium inside the interval of $(0,\pi)$, then

$$m_\theta(\theta) = \sin\theta(a' + 2b'\cos\theta) = 0 \tag{4}$$

which holds true, if

$$|2b'| > |a'| \tag{5}$$

It is obvious that (3) and (4) are valid simultaneously when $b' < 0$. Note that the dependence of $m_\theta(\theta)$ given in Fig. 1 satisfies conditions (3) and (4). The stable position occurs not only in the point of $\theta = 0$, but also in the point of $\theta = \pi$ when (3) is fulfilled for the re-entry vehicle. The motion of the spacecraft in a neighborhood of $\theta = \pi$ cannot be allowed, because in this case the back part of the body will move towards an approach flow. A simultaneous existence of the unstable equilibrium positions and small perturbations can lead to chaos.

The role of small perturbations may play, for instance, a small dynamic asymmetry of the body or a small external torque. The rigid body with a triaxial ellipsoid of inertia possesses a small dynamic asymmetry, if its transverse inertia moments differ little from each other. Then the small dynamic asymmetry is written as

$$\varepsilon = (I_2 - I_1)/I_1 \tag{6}$$

where ε is a small parameter.

Small disturbance torque is represented as the sum of the periodic term and dissipative term

$$M_d = (\nu\cos\omega t - \delta\dot\theta)I_1 \tag{7}$$

where ν and $\delta > 0$ are small parameters, $\omega$and t are frequency and time, respectively.

Below we consider successively two separate problems of perturbed motion: the problem of a spatial motion of the body with a small asymmetry (6) and the problem of a planar motion of the body under the external torque (7).

3. The spatial motion of the asymmetrical body

3.1. Hamiltonian equations

Consider the spatial motion of the rigid body about its center of mass in an atmosphere. To suppose that the biharmonic torque acts on the rigid body

$$m_\theta = aI_1\sin\theta + bI_1\sin 2\theta \tag{8}$$

where

$$a = a'/I_1, \quad b = b'/I_1 \tag{9}$$

Kinetic energy and potential energy of the spacecraft in this case become

$$\begin{aligned} T &= \frac{1}{2}(I_1p^2 + I_2q^2 + I_3r^2) \\ &= \frac{1}{2}\Big[I_1(\dot\phi\sin\theta\sin\psi + \dot\theta\cos\psi)^2 \\ &\quad + I_2(\dot\phi\sin\theta\cos\psi - \dot\theta\sin\psi)^2 + I_3(\dot\phi\cos\theta + \dot\psi)^2\Big] \end{aligned}$$

$$\Pi = -\int M_\theta d\theta = aI_1\cos\theta + bI_1\cos^2\theta$$

where (p,q,r) are rotation components in the body frame and (ϕ,ψ,θ) are Euler angles. Then the Hamiltonian is

$$\begin{aligned} H = T + \Pi &= \frac{\left[(p_\phi - p_\psi\cos\theta)\sin\psi + p_\theta\sin\theta\cos\psi\right]^2}{2I_1\sin^2\theta} \\ &+ \frac{\left[(p_\phi - p_\psi\cos\theta)\cos\psi - p_\theta\sin\theta\sin\psi\right]^2}{2I_2\sin^2\theta} \\ &+ \frac{p_\psi^2}{2I_3} + aI_1\cos\theta + bI_1\cos^2\theta. \end{aligned} \tag{10}$$

where $(p_\phi = \partial T/\partial\phi, \quad p_\psi = \partial T/\partial\psi, \quad p_\theta = \partial T/\partial\theta)$ are the generalized momentums and (θ,ψ,ϕ) are the generalized coordinates.

The Hamiltonian (10) can be written as

$$H = H^0 + \varepsilon H^1 + O(\varepsilon^2) \tag{11}$$

where

$$H^0 = \frac{p_\theta^2}{2I_1} + \frac{(p_\phi - p_\psi\cos\theta)^2}{2I_1\sin^2\theta} + \frac{p_\psi^2}{2I_3} + aI_1\cos\theta + bI_1\cos^2\theta \tag{12}$$

$$H^1 = -\frac{\left[(p_\phi - p_\psi\cos\theta)\cos\psi - p_\theta\sin\theta\sin\psi\right]^2}{2I_1\sin^2\theta} \tag{13}$$

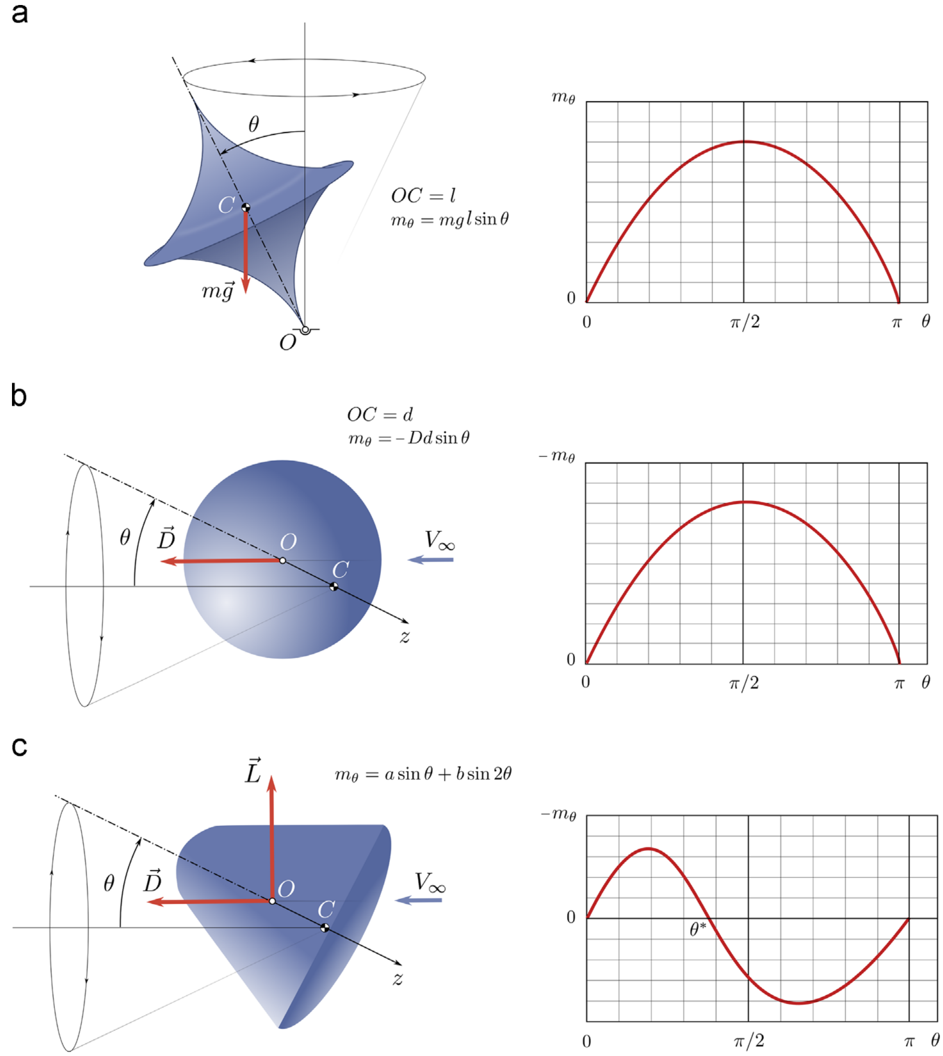

Fig. 1. Heavy body with a fixed point (a), a spherical body (b) and a blunt conical body (c) in a resisting medium.

Using the Hamiltonian equation (10), the canonical equations of the disturbed motion are [22]

$$\dot{q}_i = \frac{\partial H}{\partial p_i}, \quad p_i = -\frac{\partial H}{\partial q_i} \tag{14}$$

where$p_i = (p_\phi, p_\psi, p_\theta)$, $q_i = (\theta, \psi, \phi)$.

We note that for $b = 0$ and $\varepsilon = 0$ the Hamiltonian equation (11) corresponds to the motion of a heavy symmetrical top with one point fixed – Lagrange's case [23].

3.2. Saddle points

To get the conditions of existence of a hyperbolic point in the space $(\theta,\ p_\theta)$, consider an unperturbed canonical system for $\varepsilon = 0 (I_1 = I_2)$, using the Hamiltonian equation (12)

$$\dot{\theta} = \frac{\partial H^0}{\partial p_\theta} = \frac{p_\theta}{I_1} \tag{15}$$

$$\dot{p}_\theta = -\frac{\partial H^0}{\partial \theta} = -\frac{(p_\psi - p_\phi \cos\theta)(p_\phi - p_\psi \cos\theta)}{I_1 \sin^3\theta} + aI_1 \sin\theta + bI_1 \sin 2\theta \tag{16}$$

$$\dot{\psi} = \frac{\partial H^0}{\partial p_\psi} = \frac{p_\psi}{I_3} - \frac{(p_\phi - p_\psi \cos\theta)\cos\theta}{I_1 \sin^2\theta} \tag{17}$$

$$\dot{p}_\psi = -\frac{\partial H^0}{\partial \psi} = 0 \Rightarrow p_\psi = const \tag{18}$$

$$\dot{\phi} = \frac{\partial H^0}{\partial p_\phi} = \frac{p_\phi - p_\psi \cos\theta}{I_1 \sin^2\theta} \tag{19}$$

$$\dot{p}_\phi = -\frac{\partial H^0}{\partial \phi} = 0 \Rightarrow p_\phi = const \tag{20}$$

where $q = (\theta, \psi, \phi)$ are the generalized coordinates (the Euler angles) and $p = (p_\theta, p_\psi, p_\phi)$ are the generalized momentums.

The Hamiltonian equation (12) can be reduced to the equation of the form [13]

$$\frac{\dot{\theta}^2}{2} + \frac{\overline{p}_\phi^2 + \overline{p}_\psi^2 - 2\overline{p}_\phi \overline{p}_\psi \cos\theta}{2\sin^2\theta} + a\cos\theta + b\cos^2\theta = E = const \tag{21}$$

where $\overline{p}_\psi = p_\psi / I_1$ and $\overline{p}_\phi = p_\phi / I_1$. The variable substitution $u = \cos\theta$ in Eq. (21) gives

$$\frac{\dot{u}^2}{2(1-u^2)} + W(u) = E, \tag{22}$$

where

$$W(u) = W_g(u) + W_r(u), \quad W_g(u) = \frac{\overline{p}_\phi^2 + \overline{p}_\psi^2 - 2\overline{p}_\phi \overline{p}_\psi u}{2(1-u^2)},$$

$$W_r(u) = au + bu^2.$$

To study the behavior of the function $W(u)$ for different combinations of the parameters $\bar{p}_\psi$, $\bar{p}_\phi$, a and b, we first find the derivative of the function $W_g(u)$ with respect to the variable u

$$W_g''(u) = \frac{\left(\bar{p}_\phi^2 + \bar{p}_\psi^2\right)u - \bar{p}_\phi \bar{p}_\psi (1+u^2)}{(1-u^2)^2}$$

The numerator of the fraction has real mutually inverse roots $\bar{p}_\phi/\bar{p}_\psi$ and $\bar{p}_\psi/\bar{p}_\phi$, only one of which belongs to the interval $-1 < u = \cos\theta < 1$. Consequently, a unique extremum of the function $W_g(u)$ exists, where this extremum, equal to $\max(\bar{p}_\psi{}^2, \bar{p}_\phi{}^2)/2 \geq 0$, is obviously a minimum. Analyzing the second derivative

$$W_g''(u) = \frac{\left(\bar{p}_\phi^2 + \bar{p}_\psi^2\right)(1+3u^2) - 2\bar{p}_\phi \bar{p}_\psi u(3+u^2)}{(1-u^2)^3}$$

we can establish that it, like the function $W_g(u)$ itself, is non-negative on the interval $(-1, 1)$.

Indeed, the numerator has extreme value in the already known points $\bar{p}_\phi/\bar{p}_\psi$ and $\bar{p}_\psi/\bar{p}_\phi$, equal to $(\bar{p}_\psi{}^2 - \bar{p}_\phi{}^2)^2/\bar{p}_\phi{}^2 \geq 0$ и $(\bar{p}_\psi{}^2 - \bar{p}_\phi{}^2)^2/\bar{p}_\psi{}^2 \geq 0$, respectively, while at the ends of the interval $u = \pm 1$ it has the values $4(\bar{p}_\psi \mp \bar{p}_\phi)^2 \geq 0$. Hence it follows that the function $W_g(u)$ has no points of inflection, and its derivative increases monotonically over the whole interval.

Now we consider the quadratic function $W_r(u)$. It has an extremum at the point $(-a/2b)$, where its derivative $W_r'(u) = a + 2bu$ is equal to zero. The second derivative $W_r''(u) = 2b$ is a constant quantity. It follows from this that when the condition

$$b \geq -\min_{-1 \leq u \leq 1} [0.5 W_g''(u)] \equiv b^* \tag{23}$$

the second derivative $W''(u)$ is non-negative and function $W(u)$ on the interval $(-1, 1)$ has no inflection points. This means that there is a unique stable equilibrium position on the phase portrait of the system, and there is no singular saddle point. Saddle point is also absent if

$$|b| \leq 0.5|a| \tag{24}$$

In this case $W_r'(u)$ has the same sign over the whole section and consequently $W'(u) = 0$ at a single point, and the function $W(u)$ has a unique extremum – a minimum. If none of the conditions (23) and (24) is not satisfied, then two minima and a single maximum of the function $W(u)$ exist in the interval $(-1, 1)$. It corresponds to the presence of the phase portrait of an unstable singular saddle-type point. This situation takes place when the following condition is satisfied

$$W'(u_{*1})W'(u_{*2}) < 0 \tag{25}$$

where u_{*1}, u_{*2} are the roots of the equation $W''(u) = 0$. When condition (25) is satisfied, the phase plane is separated by the separatrices into the following three areas: an outer area A_0 and two inner areas A_1 and A_2 (Fig. 2).

Thus, if there is a saddle in the phase portrait, then from the condition (23) follows:

$$b < 0 \tag{26}$$

3.3. Homoclinic orbits

To find the two homoclinic orbits for the areas A_1 and A_2 (Fig. 2), which intersect in the saddle $u = u_0$, Eq. (22) can be solved with respect to

$$\dot{u}^2 = 2(1-u^2)(E - au - bu^2) + 2\bar{p}_\psi \bar{p}_\phi u - \bar{p}_\psi{}^2 - \bar{p}_\phi{}^2 = f(u) \tag{27}$$

In general, the degree of the polynomial $f(u)$ equals four. For the particular case $E = W_0$ as indicated in Fig. 2, which is the motion along the separatrices (the homoclinic orbits) the degree

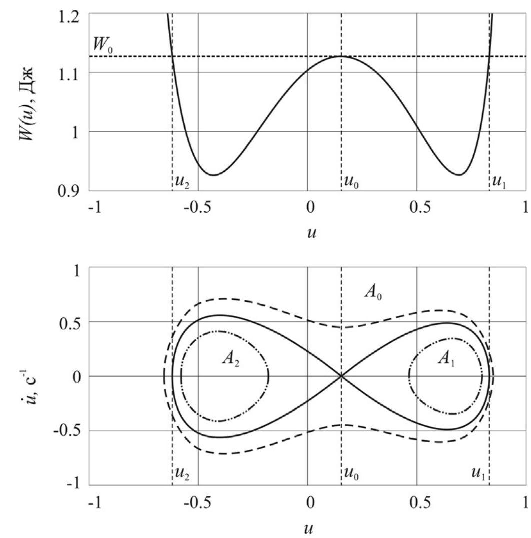

Fig. 2. Phase portraits.

of the polynomial is three

$$f(u) = -2b(u-u_0)^2(u_1-u)(u-u_2) = \dot{u}^2 \tag{28}$$

where $-1 > u_2 > u_0 > u_1 > 1$ are the roots of the polynomial as shown in Fig. 2. Separating the variables in (28) and integrating it, we get

$$\sqrt{-2b} \cdot t = \int \frac{du}{(u-u_0)\sqrt{(u_1-u)(u-u_2)}} + D \tag{29}$$

where $b < 0$ see (26) and D is an arbitrary constant. Substituting the variables $u = x + u_0$, we present this integral to a well known form [24]

$$\sqrt{-2b} \cdot t = \int \frac{dx}{x\sqrt{R(x)}} + D = -\frac{1}{\sqrt{\alpha}} \ln \frac{2\alpha + \beta x + 2\sqrt{\alpha R(x)}}{x} + D \tag{30}$$

where $\alpha = -(u_1 - u_0)(u_2 - u_0) > 0$, $\beta = u_1 + u_2 - 2u_0$, $R(x) = \alpha + \beta x - x^2$. Solving Eq. (30) for $u = x + u_0$, we obtain the two homoclinic orbits

$$cos\theta^{(j)}(t) = u_0 - \frac{4\alpha}{2\beta - (4\alpha + \beta^2)C_j{}^{-1}\exp(\lambda t) - C_j \exp(-\lambda t)}, \quad (j = 1, 2) \tag{31}$$

where

$$\lambda = \sqrt{2b(u_1 - u_0)(u_2 - u_0)},$$

$$C_j = \frac{2\alpha + \beta(u_j - u_0) + 2\sqrt{\alpha[\alpha + \beta(u_j - u_0) - (u_j - u_0)^2]}}{u_j - u_0}$$

The arbitrary constants C_j are found for the following initial conditions:

$$t = 0: \ \theta_0 = \arccos(u_j), \quad \dot{\theta}_0 = 0, \quad (j = 1, 2)$$

3.4. Melnikov function

For the small body asymmetry, when $\varepsilon = (I_2 - I_1)/I_1 \neq 0$ the behavior of the asymmetry body differs significantly from the motion of the symmetrical body (i.e., for $I_2 = I_1$). There is the additional small term (13) in the Hamiltonian equation (11) which depends on angle ψ. This perturbation leads to the destruction of the separatrices of unperturbed system of Eqs. (15)–(20) and the formation of a stochastic layer even for small values of $\varepsilon = (I_2 - I_1)/I_1$. The homoclinic trajectories corresponding to the motion along the separatices are needed to use the Melnikov method [25] that shows the distance between the stable and unstable manifolds. There are transverse intersections between the stable and unstable manifolds of hyperbolic trajectories, if the Melnikov function has simple zeroes. We use the modified Melnikov method developed by Holmes and Marsden [15]. The Melnikov function is given by

$$M(\psi_0)=\int_{-\infty}^{\infty}G(t,\psi_0)dt, \tag{32}$$

$$G=\left\{H^0,\frac{H^1}{\Omega}\right\}_{\theta,p_\theta}=\frac{1}{\Omega}\left\{H^0,H^1\right\}_{\theta,p_\theta}-\frac{H^1}{\Omega^2}\left\{H^0,\Omega\right\}_{\theta,p_\theta} \tag{33}$$

where { , } is Poisson bracket. We have from [13] and (17)

$$\left\{H^0,H^1\right\}_{\theta,p_\theta}=\frac{\partial H^0}{\partial\theta}\frac{\partial H^1}{\partial p_\theta}-\frac{\partial H^0}{\partial p_\theta}\frac{\partial H^1}{\partial\theta},\quad \left\{H^0,\Omega\right\}_{\theta,p_\theta}=-\frac{\partial H^0}{\partial p_\theta}\frac{\partial\Omega}{\partial\theta} \tag{34}$$

$$\Omega(\theta(t))=\frac{\partial H^0}{\partial p_\psi}=\frac{p_\psi}{I_3}-\frac{(p_\phi-p_\psi\cos\theta(t))\cos\theta(t)}{I_1\sin^2\theta(t)} \tag{35}$$

and compute that

$$\frac{\partial H^0}{\partial p_\theta}=\frac{p_\theta}{I_1}=\dot{\theta}, \tag{36}$$

$$\frac{\partial H^0}{\partial\theta}=\frac{(p_\phi-p_\psi\cos\theta)(p_\psi-p_\phi\cos\theta)}{I_1\sin^3\theta}-aI_1\sin\theta-bI_1\sin 2\theta \tag{37}$$

$$\frac{\partial H^1}{\partial p_\theta}=\frac{(p_\phi-p_\psi\cos\theta)\cos\psi-p_\theta\sin\theta\sin\psi}{I_1\sin\theta}\sin\psi \tag{38}$$

$$\frac{\partial H^1}{\partial\theta}=-\frac{(p_\phi-p_\psi\cos\theta)\cos\psi-p_\theta\sin\theta\sin\psi}{I_1\sin^3\theta}(p_\psi-p_\phi\cos\theta)\cos\psi \tag{39}$$

$$\frac{\partial\Omega}{\partial\theta}=\frac{p_\phi(1+\cos^2\theta)-2p_\psi\cos\theta}{I_1\sin^3\theta} \tag{40}$$

where $\theta(t)$ are the homoclinic orbits (31) and

$$\psi(t)=\int_0^t\Omega(\theta(t))dt+\psi_0=\overline{\psi}(t)+\psi_0 \tag{41}$$

Substituting Eqs. (34)–(41) into (33) can be written as

To show that transverse homoclinic orbits occur for $\varepsilon\neq 0$ we need only to prove that the Melnikov function (32) has simple zeroes. We expand the expression (42) in trigonometric series in the variable ψ_0 and using the symbol manipulator Mathematics [26] can be shown that only one term for $\sin 2\psi_0$ is an even function of t. Then the Melnikov function (32) can be written as

$$M(\psi_0)=\left[\int_{-\infty}^{\infty}R(t)dt\right]\sin 2\psi_0=P\sin 2\psi_0 \tag{43}$$

where $R(t)$ are the even known functions of t, which has a cumbersome form. Obviously, the function has simple zeroes and this result agrees with the analysis given by [15].

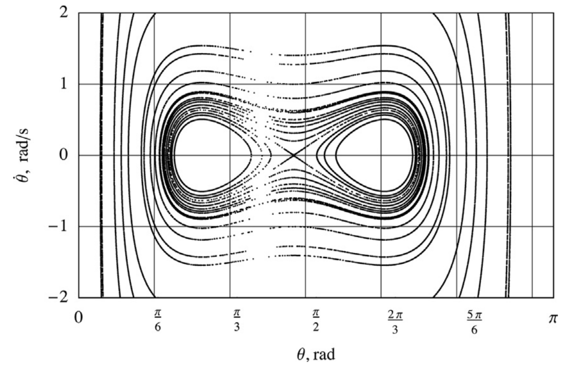

Fig. 3. Poincare section of the perturbed system for $\varepsilon=0$.

3.5. Numerical analyses for spatial motion

In order to check the validity of the analytical criterion given by (43), several numerical techniques are used. They are based on the numerical integration of the equations of the disturbed motion (14). We use the Poincare cross-section method, examining manifolds with plane sections, perpendicular to the phase axis ψ in the two-dimensional space (θ,p_θ) divided with an interval of 2π. In all the calculations the biharmonic torque coefficients, the moments of inertia and initial conditions are assumed to be as follows:

$$a=1,\quad b=-2,\quad I_1=1\text{ kg m}^2,\quad I_3=1.5\text{ kg m}^2$$

$$p_\theta=0,\quad p_\psi=1\text{ kg m}^2\text{c}^{-1},\quad p_\phi=1.4\text{ kg m}^2\text{c}^{-1},$$

$$\theta=1.4212,\quad \psi=0,\quad \phi=0 \tag{44}$$

The roots of the polynomial (28), corresponding to the motion along separatrices are

$$u_2=-0.626,\quad u_0=0.149,\quad u_1=0.828$$

For the parameters (44) the factor of the Melnikov function (43)

$$P=\int_{-\infty}^{\infty}R(t)dt$$

computed along the separatrices bounding areas A_1 and A_2 (Fig. 2) are equal, respectively, to

$$P_1=4192.86,\quad P_2=-1.77$$

At $\varepsilon=0$ the regular structure of phase space is observed (Fig. 3), trajectories have no crossings, and Poincare sections coincide with undisturbed phase portrait. The small perturbations ($\varepsilon=0.05$) lead to a complication of the phase space and occurrence of a chaotic layer near the undisturbed separatrices. The intersection of stable and unstable manifolds in the homoclinic orbits is revealed in the Poincare plane of Fig. 4. Therefore, the occurrence of chaos in the perturbed system is verified.

$$\begin{aligned}G(t,\psi_0)=\frac{I_3}{4I_1}\Bigg[&\frac{I_3p_\theta\csc\theta(p_\phi(3+\cos 2\theta)-4p_\psi\cos\theta)\left[p_\theta\sin\theta\sin(\overline{\psi}+\psi_0)+(p_\psi\cos\theta-p_\phi)\cos(\overline{\psi}+\psi_0)\right]}{I_3\cot\theta\csc\theta(p_\psi\cos\theta-p_\phi)+I_1p_\psi}\\&-2\Big[2(p_\phi\cos\theta-p_\psi)p_\theta\sin\theta\cos(\overline{\psi}+\psi_0)+\Big(2I_1^2(a+2b\cos\theta)\sin^4\theta+2\left(p_\psi^2+p_\phi^2\right)\cos\theta\\&-(3+\cos 2\theta)p_\phi p_\psi\Big)\sin(\overline{\psi}+\psi_0)\Big]\Bigg]\frac{\csc^4\theta(p_\theta\sin\theta\sin(\overline{\psi}+\psi_0)+(p_\psi\cos\theta-p_\phi)\cos(\overline{\psi}+\psi_0))}{I_3\cot\theta\csc\theta(p_\psi\cos\theta-p_\phi)+I_1p_\psi}\end{aligned} \tag{42}$$

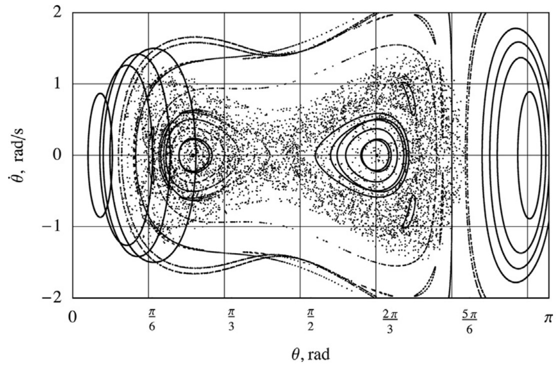

Fig. 4. Poincare section of the unperturbed system for $\varepsilon = 0.05$.

4. The planar motion of the body under the biharmonic torque and small disturbance torque

The aim of this section is to find an exact analytical representation of the Melnikov function for the planar motion, if the small disturbance is determined as the sum of a periodic time function and a dissipative torque.

4.1. The heteroclinic orbits

The plane motion of the axisymmetrical body $(p_\phi = p_\psi = 0,\ \ I_1 = I_2)$ under the disturbance torque (7) is described by one second-order differential equation

$$\ddot{\theta} = a\ \sin\ \theta + b\ \sin\ 2\theta + \nu\ \cos\ \omega t - \delta\dot{\theta} \tag{45}$$

where ν and $\delta > 0$ are small parameters. If the disturbances are absent $\nu = \delta = 0$, and we have the undisturbed system

$$\ddot{\theta} = a\ \sin\ \theta + b\ \sin\ 2\theta \tag{46}$$

Note that Eq. (46) can be interpreted as an expanded form of the Duffing equation, which is often chosen as an equation of an unperturbed motion to illustrate possibilities for using the Melnikov method, for instance [27]. To show that for small values θ Eq. (46) is equivalent to the Duffing equation, we should use the approximate representation $\left(\sin\ x = x - x^3/3!\right)$ for the trigonometric functions in Eq. (46)

$$\ddot{\theta} + \lambda\theta + \mu\theta^3 = 0,$$

where

$$\lambda = -(a + 2b), \quad \mu = \frac{a + 8b}{3!}.$$

Note also that Eq. (46) describes the motion of well-known mechanical system – a heavy material point on a circle, rotating about a vertical axis [28]

$$\ddot{\theta} = a\ \sin\ \theta + b\ \sin\ 2\theta\left(a = -\frac{g}{l}, \quad b = \Omega^2 > 0\right) \tag{1.9}$$

where g is the gravitational acceleration, l is the radius of the circle and Ω is the angular velocity of the circle.

Now we write the energy integral for Eq. (46)

$$\tfrac{1}{2}\dot{\theta}^2 + W(\theta) = E \tag{47}$$

where E is the total energy and the potential energy is

$$W(\theta) = a\ \cos\ \theta + b\cos^2\theta \tag{48}$$

If conditions (3) and (5) are satisfied (see also (9)), then the undisturbed system (46) has four equilibrium positions at $\theta \in [-\pi, \pi]$: two stable – center type

$$\theta = 0,\ \pi \tag{49}$$

and two unstable – saddle type

$$\theta_* = \pm\arccos\left(-\frac{a}{2b}\right), \tag{50}$$

where $b < 0$. The center $\theta_* = -\pi$ coincides with the center $\theta_* = \pi$. At $\theta_* \to -\pi$ and at $\theta_* \to \pi$ the speeds $\dot{\theta}$ coincide, therefore we can say that phase trajectories are closed on a cylindrical phase space. We consider the evolution of the cylindrical space in the range $\theta \in [-\pi, \pi]$. We separate two areas A_0 and A_1, divided by the two saddles s_1 and s_{-1} (Fig. 5). It is necessary to note that the area A_1 of the development of the cylinder undergoes a break at $\theta = \pi,\ \ -\pi$. From (50) it follows that if the coefficient a is equal to 0, the saddle s_1 is in the position: $\theta_* = \pi/2$. At positive values of the coefficient $a > 0$ the saddle s_1 belongs to the interval $\theta_* \in (0,\ \pi/2)$, and at negative values $a < 0$ the saddle s_1 belongs to the interval $\theta_* \in (\pi/2,\ \pi)$ (Fig. 5). Let us denote the value of the potential energy in the saddle (50) as $W_* = W(\theta_*)$. Now if $E > W_*$, then the motion is possible in the outer areas (Fig. 5). In the opposite case $(E < W_*)$ the motion can occur in any of the inner areas, depending on initial conditions. The equality $E = W_*$ corresponds to the motion along separatrixes.

Heteroclinic trajectories can be found by separation of variables in (48) and integrating it using the change of variables $x = \ \tan(\theta/2)$. As a result, we get [21]:

a) The area A_0

$$\begin{aligned} &\theta_+(t) = 2\arctan\left[\tan\frac{\theta_*}{2}\tanh\left(\frac{\lambda t}{2}\right)\right], \\ &\sigma_+(t) = (\dot{\theta}) = \frac{\lambda\ \sin\ \theta_*}{\cosh(\lambda t) +\ \cos\ \theta_*}, \\ &[\theta_-(t),\ \sigma_-(t)] = [-\theta_+(t),\ -\sigma_+(t)], \end{aligned} \tag{51}$$

b) the area A_1

$$\begin{aligned} &\theta_+(t) = \pi - 2\arctan[\cot\frac{\theta_*}{2}\tanh(\frac{\lambda t}{2})], \\ &\sigma_+(t) = (\dot{\theta}) = \frac{\lambda\ \sin\ \theta_*}{\cosh(\lambda t) -\ \cos\ \theta_*}, \end{aligned} \tag{52}$$

$$[\theta_-(t),\ \sigma_-(t)] = [2\pi - \theta_+(t),\ -\sigma_+(t)].$$

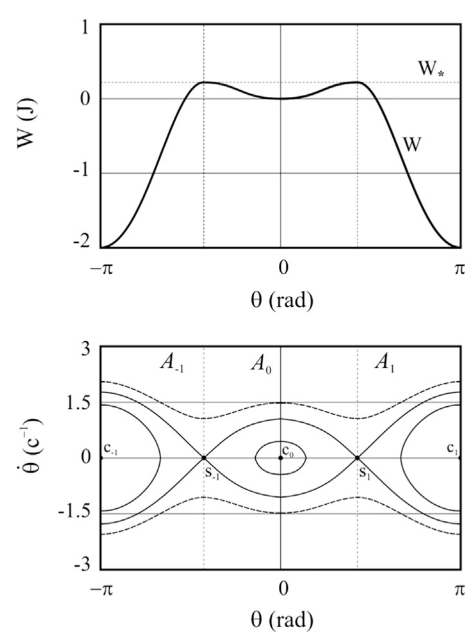

Fig. 5. The potential energy $W(\theta) = a\ \cos\ \theta + b\cos^2\theta$ and the phase space for $a = 1$, $b = -1$.

where

$$\lambda = \sqrt{\frac{a^2 - 4b^2}{2b}}.$$

4.2. The analytical Melnikov functions

The existence of heteroclinic intersections may be proved for the disturbed Eq. (45) by means of the classical Melnikov method [25]. We present a more convenient form for the application of the Melnikov method to the nonautonomous equation of the second order (45) as three differential autonomous equations of the first order [29]

$$\dot{\theta} = \sigma = f_1 + g_1$$

$$\dot{\sigma} = a \sin\theta + b \sin 2\theta + \nu \cos\phi - \delta\sigma = f_2 + g_2, \quad (53)$$

$$\dot{\phi} = \omega$$

where $f_1 = \sigma$, $g_1 = 0$, $f_2 = a \sin\theta + b \sin 2\theta$, and $g_2 = \varepsilon \cos\phi - \delta\sigma$.

The Melnikov function [23] for system (53) is given by

$$M^{\pm}(\phi_0) = \int_{-\infty}^{\infty} \{f_1[q^0_{\pm}(t)] g_2[q^0_{\pm}(t), \omega t + \phi_0]\} dt$$
$$= \nu \int_{-\infty}^{\infty} \sigma_{\pm} \cos(\omega t + \phi_0) dt - \delta \int_{-\infty}^{\infty} (\sigma_{\pm})^2 dt = M_\nu + M_\delta \quad (54)$$

where $q^0_{\pm}(t) = [\theta_{\pm}(t), \sigma_{\pm}(t)]$ are the undisturbed heteroclinic orbits (51) and (52) for the areas A_0 and A_1, respectively.

After substituting the solutions (51) and (52) into (54), the components Melnikov function M_ν and M_δ can be found in an analytical form using the tabulated integrals [30]:

a) The area A_0

$$M^{(0)}_{\nu}(\phi_0) = \nu\lambda \sin\theta_* \int_{-\infty}^{\infty} \frac{\cos(\omega t + \phi_0)}{\cosh(\lambda t) + \cos\theta_*} dt = 2\pi\nu \frac{\sinh(\theta_* \frac{\omega}{\lambda})}{\sinh(\pi \frac{\omega}{\lambda})} \cos\phi_0 \quad (55)$$

$$M^{(0)}_{\delta} = -\delta\lambda^2 \sin^2\theta_* \int_{-\infty}^{\infty} \frac{dt}{[\cosh(\lambda t) + \cos\theta_*]^2} = -2\delta\lambda[1 - \theta_* \cot\theta_*], \quad (56)$$

b) the area A_1

$$M^{(1)}_{\varepsilon}(\phi_0) = \nu\lambda \sin\theta_* \int_{-\infty}^{\infty} \frac{\cos(\omega t + \phi_0)}{\cosh(\lambda t) - \cos\theta_*} dt = 2\pi\nu \frac{\sinh((\pi - \theta_*)\frac{\omega}{\lambda})}{\sinh(\pi \frac{\omega}{\lambda})} \cos\phi_0 \quad (57)$$

$$M^{(1)}_{\delta} = -\delta\lambda^2 \sin^2\theta_* \int_{-\infty}^{\infty} \frac{dt}{[\cosh(\lambda t) - \cos\theta_*]^2} = -2\delta\lambda[1 + (\pi - \theta_*)\cot\theta_*] \quad (58)$$

It is important to note that Eqs. (55)–(58) give us analytical criteria for heteroclinic chaos in terms of the system parameters (δ, ε). Indeed, from (55)–(58) it is easy to derive that the Melnikov function (54) has simple zeroes for:

a) The area A_0

$$\delta^{(0)} < \nu \left| \frac{\pi \sinh(\theta_* \frac{\omega}{\lambda})}{\lambda[1 - \theta_* \cot\theta_*] \sinh(\pi \frac{\omega}{\lambda})} \right|, \quad (59)$$

b) the area A_1

$$\delta^{(1)} < \nu \left| \frac{\pi \sinh((\pi - \theta_*)\frac{\omega}{\lambda})}{\lambda[1 + (\pi - \theta_*)\cot\theta_*] \sinh(\pi \frac{\omega}{\lambda})} \right| \quad (60)$$

4.3. Numerical analysis for the plane motion

In order to study the influences of the small disturbances on the dynamics, the disturbed motion of the biharmonical system (45) is analyzed by constructing Poincare surfaces in the two-dimensional space $(\theta, \dot{\theta})$. In Fig. 6, at $\nu = 0$, $\delta = 0$ the regular structure of the phase space is observed, the trajectories have no intersections, and Poincaré sections coincide with undisturbed phase portrait.

The disturbances result in the complication of the phase space and the occurrence of a chaotic layer near the undisturbed separatrixes as shown in Figs. 7–8. The growth of disturbances there leads to an increase in the width of the chaotic layer, and the new oscillatory modes determined by closed curves, uncharacteristic for the undisturbed case are observed.

In order to check in a quantitative way the validity of the analytical criteria (59) and (60) we focus on the evolution of the stable and unstable manifolds associated with the saddle fixed points. The critical coefficients of the damping torque are equal to the following values:

$$\delta^{(0)} = 0.01823, \quad \delta^{(1)} = 0.00906 (\nu = 0.02)$$

Fig. 9 demonstrates numerical simulations of the phase space with initial conditions close to the undisturbed separatrixes ($\theta_0 = -1.0572$, $\dot{\theta}_0 = 0.01$, $\phi_0 = \pi/10$) in the area A_0. Now, we reset the value of δ from $\delta^{(0)} = 0.01823$ to greater ones as illustrated in Fig. 9. It can be observed clearly that, for $\delta < \delta^{(0)} (\delta = 0.018)$, the stable and unstable manifolds transversally intersect each other (Fig. 9(a)). However, when $\delta > \delta_0$ $(\delta = 0.020)$, the invariant manifolds do not intersect (Fig. 9(b)). Fig. 10 indicates similar results in the area A_1 $(\delta^{(1)} = 0.00906)$ for the following initial conditions:$\theta_0 = 0.9472$, $\dot{\theta}_0 = 0.2$, $\phi_0 = \pi$. Fig. 10(a) has been constructed for $\delta < \delta^{(1)}$ $(\delta = 0.0090)$ and Fig. 10(b) has been constructed for $\delta > \delta^{(1)}$ $(\delta = 0.0113)$. Thus the description, based on numerical simulations for some certain parameter values, makes a good match with the analytical criteria (59) and (60) provided by the Melnikov method.

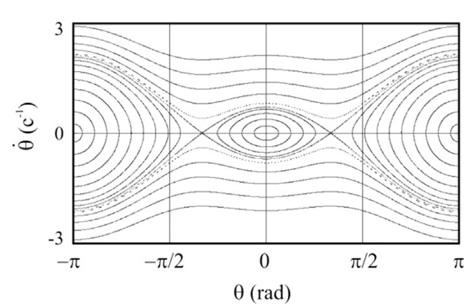

Fig. 6. Poincaré sections for $\nu = 0$, $\delta = 0$.

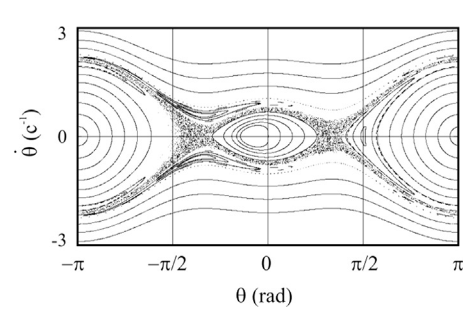

Fig. 7. Poincaré sections for $\nu = 0.02$, $\delta = 0$.

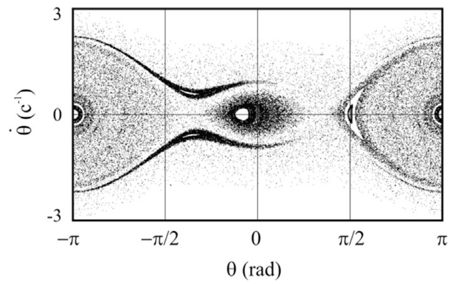

Fig. 8. Poincaré sections for $\nu = 0.02$, $\delta = 0.0001$.

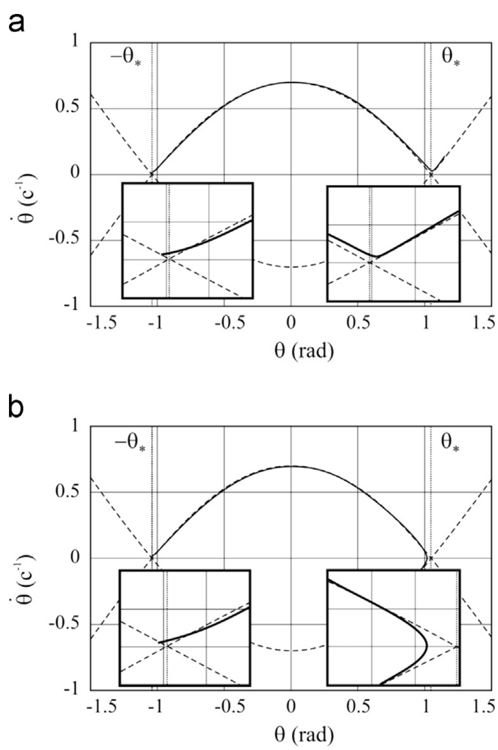

Fig. 9. Phase trajectories for $a = 1$, $b = -1$, $\nu = 0.02$, $\omega = 1$ and the two different values of δ close to the critical value $\delta^{(0)} = 0.01823$[(a) – $\delta = 0.018$ (b) – $\delta = 0.020$] with the following initial conditions: $\theta_0 = -1.0572$, $\dot{\theta}_0 = 0.01$, $\phi_0 = \pi/10$ in the area A_0[8(a) – $\delta = 0.018$, 8(b) – $\delta = 0.020$].

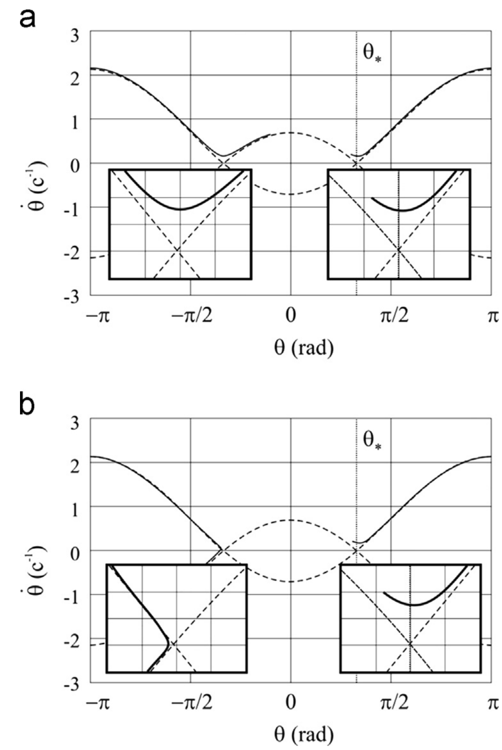

Fig. 10. Phase trajectories for $a = 1$, $b = -1$, $\nu = 0.02$, $\omega = 1$ and two different values of δ close to the critical value $\delta^{(1)} = 0.00906$, with following initial conditions: $\theta_0 = 0.9472$, $\dot{\theta}_0 = 0.2$, $\phi_0 = \pi$ for the area A_1 [9(a) – $\delta = 0.0090$, and 9(b) $\delta = 0.0113$].

5. Conclusion

The main contribution of this paper is the formulation of an approach for the study of the pitch motion dynamics of a rigid body in a resistant medium under the influence of the biharmonic torque $a \sin \theta + b \sin 2\theta$. We have suggested to introduce the biharmonic torque which reflects the behavior of the blunt-shaped spacecrafts of small elongation descended in the atmosphere. This work describes the some transient cases occurring during a spacecraft descent in a planet atmosphere using methods of chaotic mechanics, in particular, the classical Melnikov method and the modified Melnikov method developed by Holmes and Marsden. We studied two cases: the problem of a spatial motion of the body with a small dynamic asymmetry (6) and the problem of a planar motion of the body under the external torque (7) as the sum of the periodic time function and the dissipative torque. In both cases we have found the analytical solutions for the homo-heteroclinic orbits. In the first case (spatial), the criteria for chaotic motions are derived by means of the numerical computation of the Melnikov's integrals given in the quadrature. In the second case (the planar motion) we found the Melnikov function in the analytical form.

It is interesting that Eq. (53) can be represented as an extended Duffing equation, which has mechanical application in the dynamics of blunt bodies in a resisting medium. Frequently the Duffing equation is used to illustrate chaos [27,29,31,32], however, for the first time Melnikov functions are obtained in an analytical form (55)–(58) for the extended Duffing equation (53).

It is notable that all analytical and numerical results given by the Melnikov method have been confirmed by a good agreement with direct numerical calculations in the construction of Poincaré sections by using the fourth-order Runge–Kutta algorithms.

Acknowledgments

This work was supported by Ministry of Education and Science of Russia (Contract no. 9.540.2014/K)

References

[1] M. Petrović, Elementi matematičke fenomenologije (elements of mathematical phenomenology), Srpska Kraljevska Akademija, Beograd, 1911. ⟨http://elibrary.matf.bg.ac.rs/handle/123456789/476?locale-attribute=sr⟩.
[2] K.R. (Stevanović) Hedrih, A.N. Hedrih, Phenomenological mapping and dynamical absorptions in chain systems with multiple degrees of freedom, J. Vib. Control (2014), http://dx.doi.org/10.1177/1077546314525984.
[3] I.u.A. Sadov, The action-angle variables in the Euler–Poinsot problem, Akad. Nauka SSSR, Prep. 22, 1970.
[4] A. Deprit, A. Elipe, Complete reduction of the Euler–Poinsot problem, J. Astronaut. Sci. 41 (1993) 603–628.
[5] J.A. Serret, M´emoire sur l'emploi de la m´ethode de la variation des arbitraires dans la th´eorie des mouvements de rotation, M´em. Acad´. Sci. Paris 35 (1866) 585–616.
[6] H. Andoyer, Cours de m´ecanique c´eleste. Interdisciplinary Applied Mathematics, Gauthier- Villars et Cie, Paris, 1923.
[7] A. Deprit, Free rotation of a rigid body studied in the phase plane, Am. J. Phys. 35 (1967) 424–428.
[8] L.D. Akulenko, D.D. Leshchenko, F.L. Chernousko, Perturbed motions of a solid, close to Lagrange's case, Prikl. Mat. Mekhanika 43 (1979) 771–778.

[9] V.A. Yaroshevskii, Analytical estimates of peak amplitudes of oscillations of the angle of attack for uncontrolled spacecraft entering into the atmosphere: a case of plane motion, Cosm. Res. 38 (2000) 410–414.
[10] V.A. Yaroshevskii, Investigation of conditions for plane autorotation of a spacecraft entering the atmosphere, Cosm. Res. 39 (2001) 38–45.
[11] V.A. Yaroshevskii, Determination of the width of a corridor of re-entry into the atmosphere for the problem of launching a spacecraft into a circumplanetary orbit after braking in the atmosphere, Cosm. Res. 44 (2006) 236–244.
[12] V.A. Yaroshevskii, Semianalytic estimations of boundaries of a corridor of spacecraft entry into the planetary atmosphere at considerable values of permissible maximum overload, Cosm. Res. 46 (2008) 517–522.
[13] V.S. Aslanov, Spatial chaotic vibrations when there is a periodic change in the position of the centre of mass of a body in the atmosphere, J. Appl. Math. Mech. 73 (2009) 179–187.
[14] V.S. Aslanov, The motion of a rotating body in a resisting medium, Mech. Solids 40 (2005) 21–32.
[15] P.J. Holmes, J.E. Marsden, Horseshoe and Arnold diffusion for Hamiltonian system on Lie groups, Indiana Univ. Math. J. 32 (1983) 273–309.
[16] H.C. Simpson, M.D. Gunzburger, A two time analysis of gyrocopic motion with friction, J. Appl. Math. Phys. 37 (6) (1986) 867–894.
[17] D.J. Mc Gill, L.S. Long, The effect of viscous damping on spin stability of a rigid body with a fixed point, J. Appl. Mech. 44 (2) (1977) 349–352.
[18] V.V. Sidorenko, Capture and escape from resonance in the dynamics of the rigid body in viscous medium, J. Nonlinear Sci. 4 (1994) 35–57.
[19] G.H.M. van der Heijden, J.M.T. Thomson, The Chaotic instability of a slowly spinning asymmetric top, Math. Comput. Model. 36 (2002) 359–369.
[20] V. Aslanov, A. Ledkov, Analysis of the resonance and ways of its elimination at the descent of spacecrafts in the rarefied atmosphere, Aerosp. Sci. Technol. 13 (2009) 224–231.
[21] V.S. Aslanov, Chaotic behavior of the biharmonic dynamics system, Int. J. Math. Math. Sci. (2009) 2009, p. 18, (Article ID 319179), 10.1155/2009/319179.
[22] H. Goldstein, Classical Mechanics, Addison-Wesley Press, Massachusetts, 1950.
[23] W.B. Heard, Rigid Body Mechanics: Mathematics, Physics and Applications, John Wiley & Sons, Hoboken, NJ, 2008.
[24] G.A. Corn, T.M. Corn, Mathematical Handbook, McGraw-Hill, New York, 1968.
[25] V.K. Melnikov, On the stability of the center for time periodic perturbations, Moscow Math. Soc. 12 (1963) 1–56.
[26] Wolfram MathWorldive Mathematics Resource, ⟨http://mathworld.wolfram.com/⟩.
[27] F.C. Moon, Chaotic vibrations: an introduction for applied scientists and engineers. Research supported by NSF, USAF, US Navy, US Army, and IBM, Wiley-Interscience, New York, 1987.
[28] A.A. Andronov, Theory of Oscillators, Dover Publications, Mineola, New York, 1966.
[29] S. Wiggins, Introduction to Applied Nonlinear Dynamical Systems and Chaos, Springer-Verlag, New York, 2003.
[30] H. Bateman, A. Erdélyi, H. van Haeringen, L.P. Kok, Tables of Integral Transforms, McGraw-Hill, New York, 1954.
[31] J. Guckenheimer, P. Holmes, Nonlinear Oscillations, Dynamical and Bifurcations of Vector Fields, Springer-Verlag, New York, 1986.
[32] E. Simiu, Chaotic Transitions in Deterministic and Stochastic Dynamical Systems, Princeton University Press, Princeton and Oxford, 2002.